frontiers in Immunology

ORIGINAL RESEARCH
published: 06 December 2018
doi: 10.3389/fimmu.2018.02873

Expression of a Recombinant High Affinity IgG Fc Receptor by Engineered NK Cells as a Docking Platform for Therapeutic mAbs to Target Cancer Cells

Kristin M. Snyder[1], Robert Hullsiek[1], Hemant K. Mishra[1], Daniel C. Mendez[1], Yunfang Li[1], Allison Rogich[1], Dan S. Kaufman[2], Jianming Wu[1] and Bruce Walcheck[1]**

[1] Department of Veterinary and Biomedical Sciences, University of Minnesota, St. Paul, MN, United States, [2] Department of Medicine, University of California, San Diego, San Diego, CA, United States

OPEN ACCESS

Edited by:
R. Keith Reeves, Harvard Medical School, United States

Reviewed by:
Gunnur Deniz, Istanbul University, Turkey
Ahmed Lasfar, Rutgers University, The State University of New Jersey, United States

***Correspondence:**
Jianming Wu
jmwu@umn.edu
Bruce Walcheck
walch003@umn.edu

Specialty section:
This article was submitted to Molecular Innate Immunity, a section of the journal Frontiers in Immunology

Received: *27 September 2018*
Accepted: *22 November 2018*
Published: *06 December 2018*

Citation:
Snyder KM, Hullsiek R, Mishra HK, Mendez DC, Li Y, Rogich A, Kaufman DS, Wu J and Walcheck B (2018) Expression of a Recombinant High Affinity IgG Fc Receptor by Engineered NK Cells as a Docking Platform for Therapeutic mAbs to Target Cancer Cells. Front. Immunol. 9:2873. doi: 10.3389/fimmu.2018.02873

Anti-tumor mAbs are the most widely used and characterized cancer immunotherapy. Despite having a significant impact on some malignancies, most cancer patients respond poorly or develop resistance to this therapy. A known mechanism of action of these therapeutic mAbs is antibody-dependent cell-mediated cytotoxicity (ADCC), a key effector function of human NK cells. CD16A on human NK cells has an exclusive role in binding to tumor-bound IgG antibodies. Though CD16A is a potent activating receptor, it is also a low affinity IgG Fc receptor (FcγR) that undergoes a rapid downregulation in expression by a proteolytic process involving ADAM17 upon NK cell activation. These regulatory processes are likely to limit the efficacy of tumor-targeting therapeutic mAbs in the tumor environment. We sought to enhance NK cell binding to anti-tumor mAbs by engineering these cells with a recombinant FcγR consisting of the extracellular region of CD64, the highest affinity FcγR expressed by leukocytes, and the transmembrane and cytoplasmic regions of CD16A. This novel recombinant FcγR (CD64/16A) was expressed in the human NK cell line NK92 and in induced pluripotent stem cells from which primary NK cells were derived. CD64/16A lacked the ADAM17 cleavage region in CD16A and it was not rapidly downregulated in expression following NK cell activation during ADCC. CD64/16A on NK cells facilitated conjugation to antibody-treated tumor cells, ADCC, and cytokine production, demonstrating functional activity by its two components. Unlike NK cells expressing CD16A, CD64/16A captured soluble therapeutic mAbs and the modified NK cells mediated tumor cell killing. Hence, CD64/16A could potentially be used as a docking platform on engineered NK cells for therapeutic mAbs and IgG Fc chimeric proteins, allowing for switchable targeting elements and a novel cancer cellular therapy.

Keywords: FcR, ADCC, NK cell, immunotherapy, antibody

INTRODUCTION

Natural killer (NK) cells are cytotoxic lymphocytes of the innate immune system that target stressed, infected, and neoplastic cells (1). In contrast to the diverse array of receptors involved in natural cytotoxicity, human NK cells mediate ADCC exclusively through the IgG Fc receptor CD16A (FcγRIIIA) (2–4). This is a potent activating receptor and its signal transduction involves the association of the transmembrane and cytoplasmic regions of CD16A with FcRγ and/or CD3ζ (4–9). Unlike other activating receptors expressed by NK cells, the cell surface levels of CD16A undergo a rapid downregulation upon NK cell activation during ADCC and by other stimuli (10–14). CD16A downregulation also occurs in the tumor environment of patients and contributes to NK cell dysfunction (15–19). A disintegrin and metalloproteinase-17 (ADAM17) expressed by NK cells plays a key role in its downregulation by cleaving CD16A in a *cis* manner at a specific location proximal to the cell membrane upon NK cell activation (13, 14, 20).

There are two allelic variants of CD16A that have either a phenylalanine or valine residue at position 176 (position 158 if amino acid enumeration does not include the signal sequence). The CD16A-176V variant has a higher affinity for IgG (21, 22), but CD16A-176F is the dominant allele in humans (23). Clinical analyses have revealed a positive correlation between the therapeutic efficacy of tumor-targeting therapeutic mAbs and CD16A binding affinity. Patients homozygous for the CD16A valine variant (CD16A-V/V) had an improved clinical outcome after treatment with anti-tumor mAbs compared to those who were either heterozygous (CD16A-V/F) or homozygous (CD16A-F/F) for the lower affinity FcγRIIIA isoform [as reviewed in Wang et al. (4)]. These findings establish that increasing the binding affinity of CD16A for anti-tumor mAbs may lead to improved cancer cell killing.

CD64 (FcγR1) binds to monomeric IgG with 2–3 orders of magnitude higher affinity than CD16A (24–26). CD64 recognizes the same IgG isotypes as CD16A and is expressed by myeloid cells, including monocytes, macrophages, and activated neutrophils, but not NK cells (24, 26). We generated the novel recombinant receptor CD64/16A that consists of the extracellular region of human CD64 for high affinity antibody binding, and the transmembrane and intracellular regions of human CD16A for mediating NK cell signal transduction. CD64/16A also lacked the membrane proximal ADAM17 cleavage site found in CD16A. In this study, we stably expressed CD64/16A in NK92 cells, a cytotoxic human NK cell line that lacks endogenous FcγRs (27), and in induced pluripotent stem cells (iPSCs) that were then differentiated into primary NK cells. We show that in these two NK cell platforms, this novel recombinant FcγR is functional and can capture soluble monomeric IgG therapeutic mAbs that provide targeting elements for tumor cell ADCC.

MATERIALS AND METHODS

Antibodies

All mAbs to human hematopoietic and leukocyte phenotypic markers are described in **Table 1**. All isotype-matched negative control mAbs were purchased from BioLegend (San Diego, CA). APC-conjugated $F(ab')_2$ donkey anti-human or goat anti-mouse IgG (H+L) were purchased from Jackson ImmunoResearch Laboratories (West Grove, PA). The human IgG1 mAbs trastuzumab/Herceptin and rituximab/Rituxan, manufactured by Genentech (South San Francisco, CA), and cetuximab/Erbitux, manufactured by Bristol-Myers Squibb (Lawrence, NJ), were purchased through the University of Minnesota Boynton Pharmacy. Recombinant human L-selectin/IgG1 Fc chimera was purchased from R&D Systems (Minneapolis, MN).

TABLE 1 | Antibodies.

Antigen	Clone	Fluorophore	Company
CD56	HCD56	PE-CY7	BioLegend, San Diego, CA
CD3	HIT3a	PE	BioLegend
CD16	3G8	APC	BioLegend
CD16	3G8	none	Ancell, Bayport, MN
CD7	CD7-6B7	PE/CY5	BioLegend
CD336/NKp44	P44-8	APC	BioLegend
CD335/NKp46	9E2	APC	BioLegend
CD159a/NKG2A	Z199	APC	Beckman Coulter, Brea, CA
CD314/NKG2D	1D11	PerCP/Cy5.5	BioLegend
CD158a/KIR2DL1	HP-MA4	PE	BioLegend
CD158b1/KIR2DL2/L3	DX27	PE	BioLegend
CD158e1/KIR3DL1	DX9	PE	BioLegend
CD94	DX22	PE	BioLegend
CD64	10.1	APC	BioLegend
CD64	10.1	none	Ancell
CD34	561zz	PE	BioLegend
CD45	2D1	APC	BioLegend
CD43	CD43-10G7	APC	BioLegend
CD62L/L-selectin	LAM1-116	APC	Ancell

Generation of Human CD64/16A

Total RNA was isolated from human peripheral blood leukocytes using TRIzol total RNA isolation reagent (Invitrogen, Carlsbad, CA) and cDNA was synthesized with the SuperScript preamplification system (Invitrogen). The recombinant CD64/16A is comprised of human CD64 extracellular domain and CD16A transmembrane and cytoplasmic domains. PCR fragments for CD64 (885 bps) and CD16A (195 bps) were amplified from the generated cDNA. The PCR fragments were purified and mixed together with the forward primer 5′- CGG *GAA TTC* GGA GAC AAC ATG TGG TTC TTG ACA A-3′, the reverse primer 5′- CCG *GAA TTC* TCA TTT GTC TTG AGG GTC CTT TCT-3′ (underlined nucleotides are EcoR I sites), and Pfx50 DNA polymerase (Invitrogen) to generate the recombinant CD64/16A receptor. CD64/CD16A and CD16A cDNA (CD16A-176V variant) was inserted into the retroviral expression vector pBMN-IRES-EGFP and virus was generated for NK92 cell transduction, as previously described (14). For this study, the transduced NK92 cells were sorted

by flow cytometry to derive populations with homogenous expression of CD16A or CD64/16A, but consisted of a mixed clonal population to avoid the effects of random genomic integration of vector DNA in a single NK92 transductant, as we have done in previous studies (14, 20). Additionally, CD64/CD16A cDNA was inserted into a pKT2 sleeping beauty transposon vector and used along with SB100X transposase for iPSC transduction, as previously described (14). The nucleotide sequences of all constructs were confirmed by direct sequencing from both directions on an ABI 377 sequencer with ABI BigDye terminator cycle sequencing kit (Applied Biosystems, Foster City, CA).

Cells

Fresh human peripheral blood leukocytes from plateletpheresis were purchased from Innovative Blood Resources (St. Paul, MN). Peripheral blood mononuclear cells were further enriched using Ficoll-Paque Plus (GE Healthcare Bio-Sciences AB, Uppsala, Sweden) and NK cells were purified by negative depletion using an EasySep human NK cell kit (StemCell Technologies, Cambridge, MA), as per the manufacturer's instructions, with >95% viability and 90–95% enrichment of $CD56^+CD3^-$ lymphocytes. Viable cell counting was performed using a Countess II automated cell counter (Life Technologies Corporation, Bothell, WA). The human NK cell line NK92 and the ovarian cancer cell line SKOV-3 were obtained from ATCC (Manassas, VA) and cultured per the manufacturer's directions. The NK92 cells required IL-2 for growth (500 IU/ml), which was obtained from R&D Systems and the National Cancer Institute, Biological Resources Branch, Preclinical Biologics Repository (Frederick, MD). Heat inactivated Gibco FBS was purchased from Thermo Fisher Scientific (Waltham, MA), and heat inactivated horse serum was purchased from Sigma-Aldrich (St. Louis, MO). For all assays described below, cells were used when in log growth phase.

The iPSCs UCBiPS7, derived from umbilical cord blood CD34 cells, have been previously characterized and were cultured and differentiated into hematopoietic progenitor cells as described with some modifications (14, 28–31). iPSC culture and hematopoietic differentiation was performed using TeSR-E8 medium and a STEMdiff Hematopoietic Kit (StemCell Technologies), which did not require the use of mouse embryonic fibroblast feeder cells, TrypLE adaption, spin embryoid body formation, or $CD34^+$ cell enrichment. To passage iPSCs, cells were dissociated with Gentle Cell Dissociation Reagent (StemCell Technologies) and aggregates $\geq$50 μm in diameter were counted with a hemocytometer and diluted to 20–40 aggregates/ml with TeSR-E8 medium. Each well of a 12-well plate was pre-coated with Matrigel Matrix (Corning Inc., Tewksbury, MA) and seeded with 40–80 aggregates in 2 ml of TeSR-E8 medium. Cell aggregates were cultured for 24 h before differentiation with the STEMdiff Hematopoietic Kit, as per the manufacturer's instructions. At day 12 of hematopoietic progenitor cell differentiation, the percentage of hematopoietic progenitor cells was determined using flow cytometric analysis with anti-CD34, anti-CD45, and anti-CD43 mAbs. NK cell differentiation was performed as previously described (32). The iPSC-derived NK cells, referred to here as iNK cells, were expanded for examination using γ-irradiated K562-mbIL21-41BBL feeder cells at a 1:2 ratio in cell expansion medium [60% DMEM, 30% Ham's F12, 10% human AB serum (Valley Biomedical, Winchester, VA), 20 μM 2-mercaptoethanol, 50 μM ethanolamine, 20 μg/ml ascorbic Acid, 5 ng/ml sodium selenite, 10 mM HEPES, and 100–250 IU/ml IL-2 (R&D Systems)], as described previously (14, 29–31).

Cell Staining, IFNγ Quantification, and Flow Cytometric Analysis

For cell staining, 0.5×10^6-1×10^6 cells were stained with the indicated mAbs (**Table 1**) using flow buffer (dPBS containing 2.5% FBS and 0.02% sodium azide) and 1×10^4-5×10^4 cells per sample were acquired, as previously described (11, 14, 20). For controls, fluorescence minus one was used as well as appropriate isotype-matched antibodies since the cells of interest expressed FcRs. A FSC-A/SSC-A plot was used to set an electronic gate on leukocyte populations and an FSC-A/FSC-H plot was used to set an electronic gate on single cells. A Zombie viability kit was used to assess live vs. dead cells, as per the manufacturer's instructions (BioLegend).

To assess the capture of soluble trastuzumab, rituximab, cetuximab, or L-selectin/Fc chimera, transduced NK cells were incubated with 5 μg/ml of antibody for 2 h at 37°C in MEM-α basal media (Thermo Fisher Scientific) supplemented with IL-2 (200 IU/ml), HEPES (10 mM), and 2-mercaptoethanol (0.1 mM), washed with MEM-α basal media, and then stained on ice for 30 min with a 1:200 dilution of APC-conjugated $F(ab')_2$ donkey anti-human IgG (H + L). To detect recombinant human L-selectin/Fc binding, cells were stained with the anti-L-selectin mAb APC-conjugated Lam1-116. To compare CD16A and CD64/16A staining levels on NK92 cells, the respective transductants were stained with a saturating concentration of unconjugated anti-CD16 (3G8) or anti-CD64 (10.1) mAbs (5 μg/ml), washed extensively with dPBS containing 2% goat serum and 2 mM sodium azide, and then stained with APC-conjugated $F(ab')_2$ goat anti-mouse IgG (H+L). This approach was used since directly conjugated anti-CD16 and anti-CD64 mAbs can vary in their levels of fluorophore labeling. IFNγ quantification was performed by a cytometric bead-based Flex Set assay (BD Biosciences, San Jose, CA), per the manufacturer's instructions. The minimum and maximum limit of detection for the assay was 1.8 and 2,500 pg/ml, respectively. All flow cytometric analyses were performed on a FACSCelesta instrument (BD Biosciences). Data was analyzed using FACSDIVA v8 (BD Biosciences) and FlowJo v10 (Ashland, OR).

Cell-Cell Conjugation Assay and ADCC

NK92 cells used in these assays were transduced with pBMN-IRES-EGFP empty vector or vector containing CD64/16A or CD16A cDNA. For all transductants, nearly 100% of the cells expressed GFP. The NK92 transductants were initially serum-starved for 2 h at 37°C in MEM-α basal media (Thermo Fisher Scientific, Waltham, MA) supplemented with IL-2 (200 IU/ml),

HEPES (10 mM), and 2-mercaptoethanol (0.1 mM). SKOV-3 cells were labeled with CellTrace Violet (Molecular Probes, Eugene, OR) per the manufacturer's instructions, incubated with 5 μg/ml trastuzumab for 30 min and washed with MEM-α basal media. NK92 cells and SKOV-3 cells were then resuspended in the supplemented MEM-α basal media at 1×10^6 and 2×10^6/ml, respectively. For a 1:2 Effector:Target (E:T) ratio, 100 μl of each cell type was mixed together, centrifuged for 1 min at 20 × g and incubated at 37°C for the indicated time points. After each time point, the cells were gently vortexed for 3 s and immediately fixed with 1% paraformaldehyde in dPBS at 4°C. Cells were immediately analyzed by flow cytometry for which 2×10^4 cells per sample were acquired for analyses. The percentage of conjugated NK cells was calculated by gating on GFP and CellTrace Violet double-positive events.

To evaluate ADCC, a DELFIA EuTDA-based cytotoxicity assay was used according to the manufacturer's instructions (PerkinElmer, Waltham, MA). Briefly, target cells were labeled with Bis(acetoxymethyl)-2-2:6,2 terpyridine 6,6 dicarboxylate (BATDA) for 30 min in their culture medium, washed in culture medium, and pipetted into a 96-well non-tissue culture-treated U-bottom plates at a density of 8×10^3 cells/well. A tumor targeting mAb was added at the indicated concentrations and NK cells were added at the indicated E:T ratios. The plates were centrifuged at 400 × g for 1 min and then incubated for 2 h in a humidified 5% CO_2 atmosphere at 37°C. At the end of the incubation, the plates were centrifuged at 500 × g for 5 min and supernatants were transferred to a 96 well DELFIA Yellow Plate (PerkinElmer) and combined with europium. Fluorescence was measured by time-resolved fluorometry using a BMG Labtech CLARIOstar plate reader (Cary, NC). BATDA-labeled target cells alone with or without therapeutic antibodies were cultured in parallel to assess spontaneous lysis and in the presence of 2% Triton-X to measure maximum lysis. ADCC for each sample is represented as Percent Specific Release and was calculated using the following formula:

$$Percent\ Specific\ Release = \frac{(Experimental\ release - Spontaneous\ release)}{(Maximal\ release - Spontaneous\ release)} * 100$$

For each experiment, measurements were conducted in triplicate using two-three replicate wells.

Statistical Analyses

Statistical analyses were performed by use of GraphPad Prism (GraphPad Software, La Jolla, CA, USA). After assessing for approximate normal distribution, all variables were summarized as mean ± *SD*. Comparison between 2 groups was done with Student's *t*-test, with $p < 0.05$ taken as statistically significant.

RESULTS

Expression and Function of CD64/16A in NK92 Cells

We engineered a recombinant FcγR that consists of the extracellular region of human CD64 and the transmembrane and cytoplasmic regions of human CD16A, referred to as CD64/16A (**Figure 1A**). The human NK cell line NK92 stably expressing this recombinant receptor were initially used to examine its function. These cells lack endogenous FcγRs but can mediate ADCC when expressing recombinant CD16A (14, 20, 27). As shown is **Figure 1B**, NK92 cells expressing CD64/16A were positively stained by an anti-CD64 mAb, whereas parental NK92 cells or NK92 cells expressing CD16A were not. CD16A is known to undergo ectodomain shedding upon NK cell activation resulting in its rapid downregulation in expression (10–13, 20). CD16A as well as its isoform CD16B on neutrophils is cleaved by ADAM17 (10), and this occurs at an extracellular region proximal to the cell membrane (13, 14). The ADAM17 cleavage region of CD16A is not present in CD64 or CD64/16A (**Figure 1A**). We found that CD16A underwent a >50% decrease in expression upon NK92 stimulation by ADCC, whereas CD64/16A demonstrated little to no downregulation (**Figure 1C**).

To establish the functional activity of CD64/16A, we determined its ability to promote E:T conjugation, induce ADCC, and stimulate IFN-γ production. SKOV-3 cells, an ovarian cancer cell line that expresses HER2, were used as the target. A two-color flow cytometric approach was used to quantify the conjugation of NK92-CD64/16A cells and SKOV-3 cells in the absence and presence of the anti-HER2 therapeutic mAb trastuzumab. A bicistronic vector was used for CD64/16A as well as GFP expression, and its fluorescence was used to identify the NK92 cells. SKOV-3 cells were labeled with the fluorescent dye CellTrace Violet. The incubation of NK92-CD64/16A cells with SKOV-3 cells alone resulted in a low level of conjugation after 60 min of exposure (**Figure 2A**). E:T conjugation was markedly increased in the presence of trastuzumab, and this was effectively disrupted by the presence of the anti-CD64 mAb 10.1 (**Figure 2A**), which blocks IgG binding (33). The addition of trastuzumab, however, did not enhance E:T conjugation by NK92 cells transduced with an empty vector expressing only GFP (NK92 control cells) (**Figure 2A**).

An increase in SKOV-3 cell conjugation by NK92-CD64/16A cells corresponded with increased cytolytic activity. We determined direct target cell killing by NK92-CD64/16A cells using an ADCC assay in which various concentrations of trastuzumab and E:T ratios were examined. We show in **Figure 2B** effective SKOV-3 cytotoxicity by NK92-CD64/16A cells in the presence of trastuzumab that decreased with lower mAb concentrations and lower E:T ratios. To confirm the role of CD64/16A in the induction of target cell killing, we also performed the assay in the presence the anti-CD64 mAb 10.1, which effectively blocked ADCC (**Figure 2C**).

Cytokine production is also induced during ADCC and NK cells are major producers of IFNγ (4, 34). NK92-CD64/16A cells exposed to SKOV-3 cells and trastuzumab produced considerably higher levels of IFNγ than when exposed to SKOV-3 cells alone (**Figure 2D**). Taken together, the above findings demonstrate that the CD64 component of the recombinant receptor engages

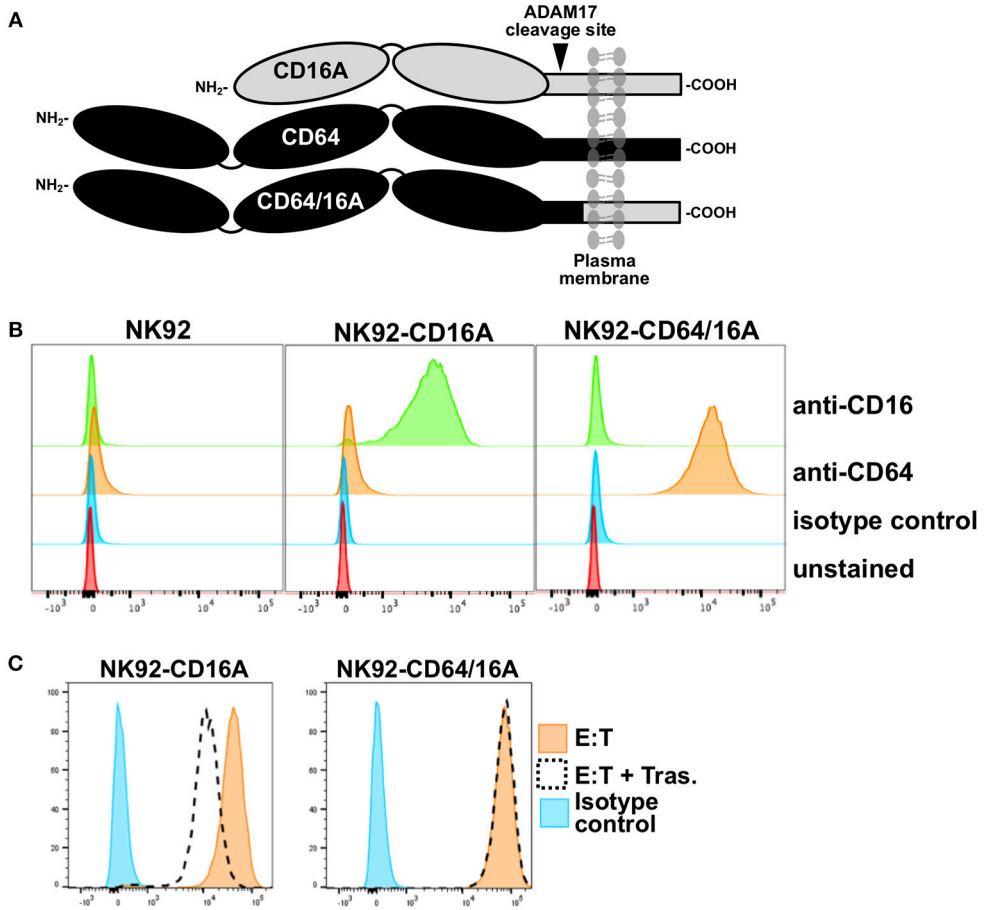

FIGURE 1 | Expression of CD64/16A by NK92 cells**. (A)** Schematic representation of the cell membrane forms of CD16A, CD64, and CD64/16A. CD16A undergoes ectodomain shedding by ADAM17 at a membrane proximal location, as indicated, which is not present in CD64 and CD64/16A. **(B)** NK92 parental cells, NK92-CD16A cells, and NK92-CD64/16A cells were stained with an anti-CD16, anti-CD64, or an isotype-matched negative control mAb and examined by flow cytometry. **(C)** NK92-CD16A and NK92-CD64/16A cells were incubated with SKOV-3 cells with or without trastuzumab (5 μg/ml) at 37° C (E:T = 1:1; 5 × 10^5 cells to 5 × 10^5 cells) for 2 h. The NK92-CD16A and NK92-CD64/16A cells were then stained with an anti-CD16 mAb or an anti-CD64 mAb, respectively, and examined by flow cytometry. Non-specific antibody labeling was determined using the appropriate isotype-negative control mAb. **(B,C)** Data is representative of at least three independent experiments.

tumor-bound antibody, and that the CD16A component promotes intracellular signaling leading to degranulation and cytokine production.

CD64/16A as a Docking Platform For Antibodies

CD64 is distinguished from the other FcγR members by its unique third extracellular domain, which contributes to its high affinity and stable binding to soluble monomeric IgG (26). We compared the ability of NK92 cells expressing CD64/16A or the high affinity variant of CD16A (CD16A-176V) to capture soluble therapeutic mAbs. NK92 cell transductants expressing similar levels of CD64/16A and CD16A (**Figure 3A**) were incubated with trastuzumab for 2 h. After which, excess antibody was washed away and the cells were stained with a fluorophore-conjugated anti-human IgG antibody and then evaluated by flow cytometry. As shown in **Figure 3B**, NK92-CD64/16A cells captured considerably higher levels of trastuzumab than did the NK92-CD16A cells (8.1-fold increase ± 1.3, mean ± *SD* of 3 independent experiments). In addition, the NK92-CD64/16A cells efficiently captured the tumor-targeting mAbs Erbitux/cetuximab and Rituxan/rituximab, as well as the fusion protein L-selectin/Fc (**Figure 3C**). We then tested whether NK92-CD64/16A cells with a captured tumor-targeting mAb mediated ADCC. For this assay, we compared equal numbers of NK92-CD64/16A and NK92-CD16A cells that were incubated with the same concentration of soluble trastuzumab, washed, and exposed to SKOV-3 cells. We observed that target cell killing by NK92-CD64/16A cells with captured trastuzumab was significantly higher than by these same cells in the absence trastuzumab and was far superior to NK92-CD16A cells at all E:T ratios examined (**Figure 3D**). In contrast, SKOV-3 cytotoxicity by NK92-CD16A and NK92-CD64/16A cells was not significantly different if trastuzumab was present

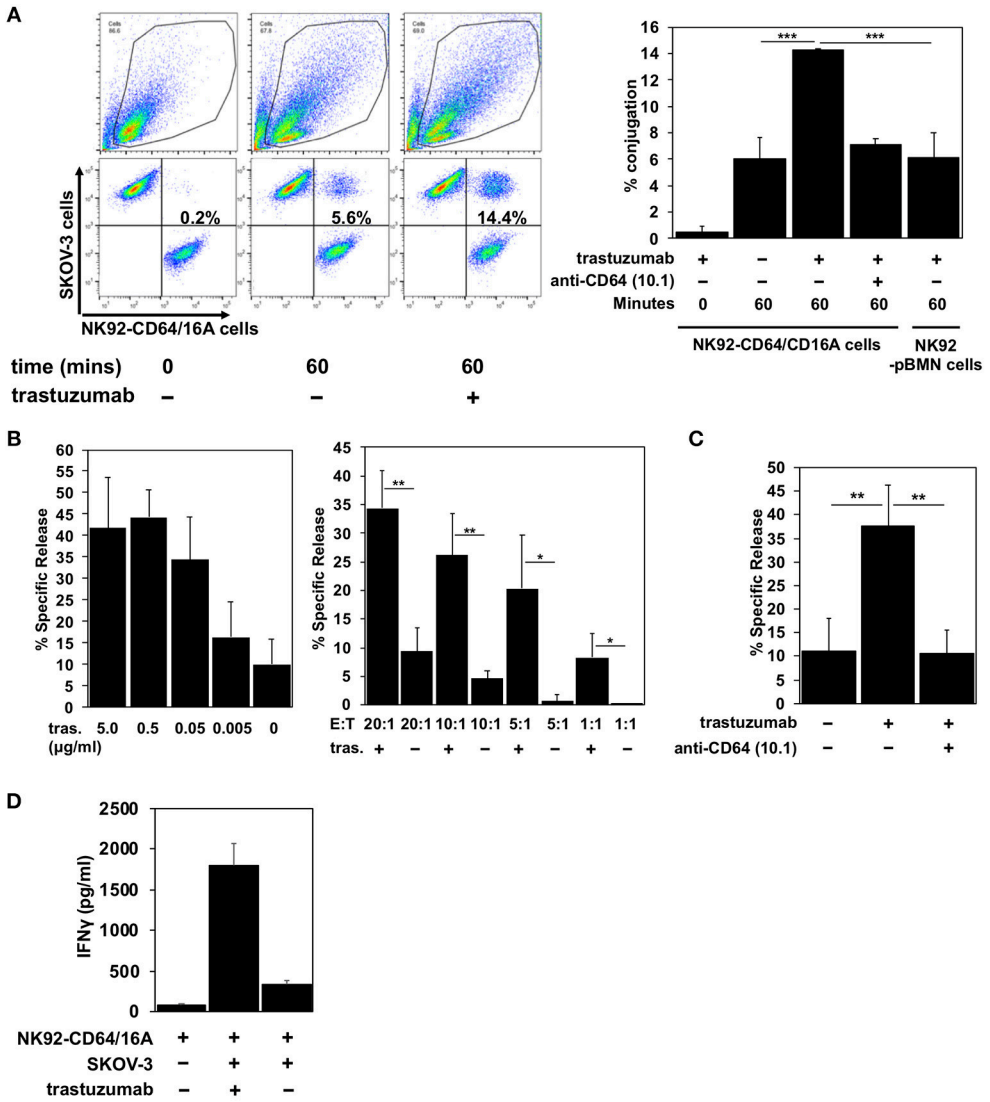

FIGURE 2 | CD64/16A promotes target cell conjugation, ADCC, and IFNγ production**. (A)** NK92 control cells or NK92-CD64/16A cells, both expressing GFP, and SKOV-3 cells, labeled CellTrace Violet, were mixed at an E:T ratio of 1:2 (1×10^5 cells to 2×10^5 cells) in the presence or absence of trastuzumab (5 µg/ml) and the anti-CD64 mAb 10.1 (10 µg/ml), incubated at 37°C up to 60 min, fixed, and then analyzed by flow cytometry, as described in the Materials and Methods. For the flow cytometric data, representative data are shown. For the bar graphs, mean ± *SD* of three independent experiments is shown. Statistical significance is indicated as ***$p < 0.001$. **(B)** NK92-CD64/16A cells were incubated with SKOV-3 cells (E:T = 20:1; 1.6×10^5 cells to 8×10^3 cells) and trastuzumab (tras.) at the indicated concentrations (left panel), or with SKOV-3 cells at the indicated E:T ratios in the presence or absence of trastuzumab (5 µg/ml) (right panel) for 2 h at 37°C. Data are represented as % specific release and the mean ± SD of 3 independent experiments is shown. Statistical significance is indicated as *$p < 0.05$, **$p < 0.01$. **(C)** NK92-CD64/16A cells were incubated with SKOV-3 cells (E:T = 20:1; 1.6×10^5 cells to 8×10^3 cells) in the presence or absence of trastuzumab (5 µg/ml) and the anti-CD64 mAb 10.1 (10 µg/ml), as indicated, for 2 h at 37°C. Data are represented as % specific release and the mean ± *SD* of 3 independent experiments is shown. Statistical significance is indicated as **$p < 0.01$. **(D)** NK92-CD64/16A cells were incubated with SKOV-3 cells (E:T = 1:1; 1×10^5 cells to 1×10^5 cells) with or without trastuzumab (5 µg/ml) for 2 h at 37°C. Secreted IFNγ levels were quantified by ELISA. Data is shown as mean of 2 independent experiments.

during the assay and not initially docked to the transductants (**Figure 3E**). This demonstrates that the different transductants had an equivalent cytolytic capacity. Taken together, these findings show that NK92 cells expressing CD64/16A can stably bind soluble anti-tumor mAbs and IgG fusion proteins, and that these can serve as targeting elements to kill cancer cells.

Expression and Function of CD64/16A in iPSC-Derived NK Cells

We also examined the function of CD64/16A in engineered primary NK cells. Genetically modifying peripheral blood NK cells by retroviral or lentiviral transduction at this point has been challenging (35). Embryonic stem cells and iPSCs can be differentiated into cytolytic NK cells *in vitro* (28–31, 36),

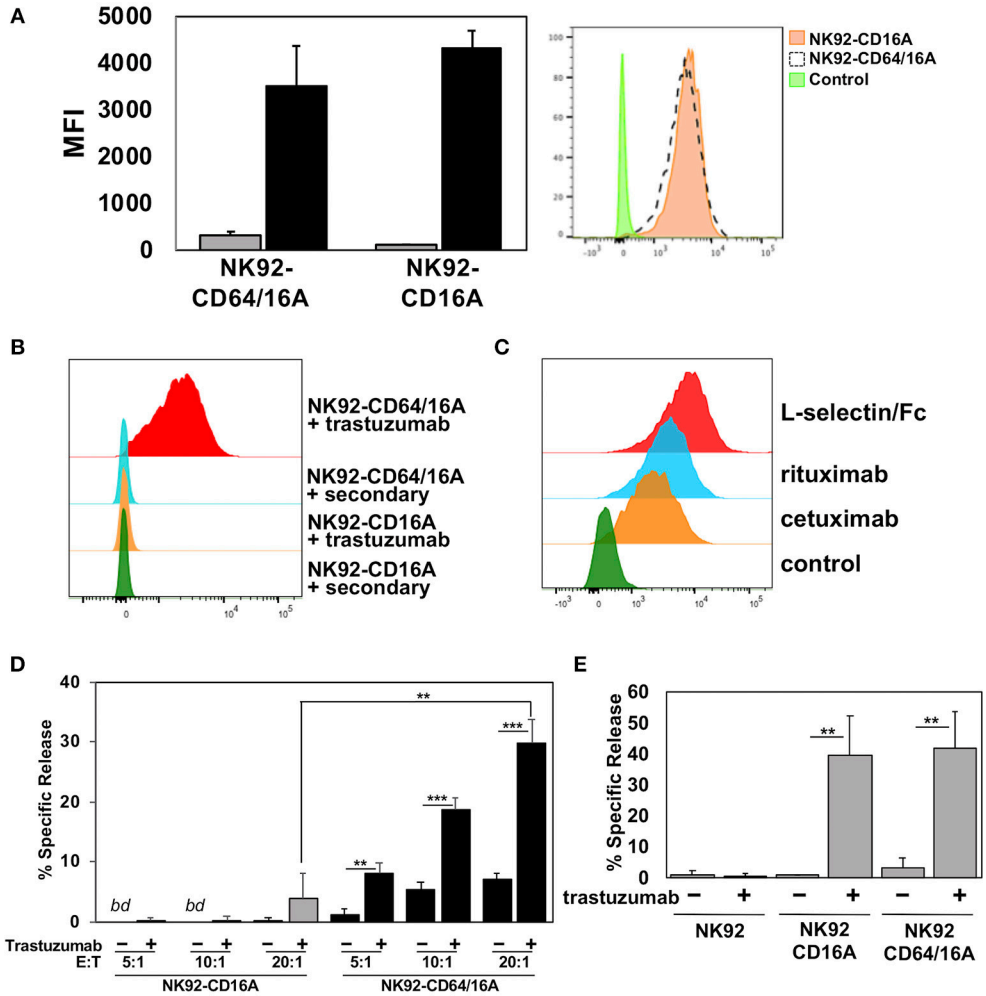

FIGURE 3 | CD64/16A attaches to soluble tumor-targeting mAbs and IgG fusion proteins**. (A)** Relative expression levels of CD16A and CD64/16A on NK92 cells were determined by cell staining with anti-CD16 and anti-CD64 mAbs (black bars), respectively, or an isotype-matched negative control antibody (gray bars). The bar graph shows mean fluorescence intensity (MFI) ± *SD* of three independent experiments. Representative flow cytometric data are shown in the histogram overlay. The dashed line histogram shows CD64 staining of NK92-CD64/16A cells, the orange-filled histogram shows CD16A staining of NK92-CD16A cells, and the green-filled histogram shows isotype control antibody staining of the NK92-CD16A cells. **(B)** NK92-CD16A and NK92-CD64/16A cells were incubated with or without trastuzumab (5 μg/ml) for 2 h at 37°C, washed, stained with a fluorophore-conjugated anti-human secondary antibody, and analyzed by flow cytometry. Data is representative of at least 3 independent experiments. **(C)** NK92-CD64/16A cells were incubated with cetuximab or rituximab (5 μg/ml for each), washed, and then stained with a fluorophore-conjugated anti-human secondary antibody. Control represents cells stained with the anti-human secondary antibody only. NK92-CD64/16A cells were also incubated with L-selectin/Fc (5 μg/ml), washed, and then stained with a fluorophore-conjugated anti-L-selectin mAb. NK92 cells lack expression of endogenous L-selectin (data not shown). All staining was analyzed by flow cytometry. Data shown are representative of 3 independent experiments. **(D)** NK92-CD16A and NK92-CD64/16A cells were incubated in the presence or absence of trastuzumab (5μg/ml), washed, and exposed to SKOV-3 cells (8×10^3) at the indicated E:T cell ratios for 2 h at 37°C. Data is shown as mean ± SD of 3 independent experiments. Statistical significance is indicated as $^{**}p < 0.01$, $^{***}p < 0.001$. *bd* = below detection, (i.e., < spontaneous release by negative control cells). **(E)** NK92-CD16A and NK92-CD64/16A cells were incubated with SKOV-3 cells (E:T = 10:1; 8×10^4 cells to 8×10^3 cells) in the presence or absence of trastuzumab (5 μg/ml), as indicated, for 2 h at 37°C. Data is shown as mean ± SD of 3 independent experiments. Statistical significance is indicated as $^{**}p < 0.01$.

and these cells are highly amendable to genetic engineering (14, 30, 37, 38). Undifferentiated iPSCs were transduced to express CD64/16A using a sleeping beauty transposon plasmid for non-random gene insertion and stable expression. iPSCs were differentiated into hematopoietic cells and then iNK cells by a two-step process that we have previously described (14, 28, 29). For this study, we modified the hematopoietic differentiation method to streamline the procedure by using a commercially available media and hematopoietic differentiation kit, as described in the Materials and Methods. $CD34^+CD43^+CD45^+$ cells were generated, further differentiated into iNK cells, and these cells were expanded for analysis using recombinant IL-2 and K562-mbIL21-41BBL feeder cells. $CD56^+CD3^-$ is a hallmark phenotype of human NK cells, and these cells

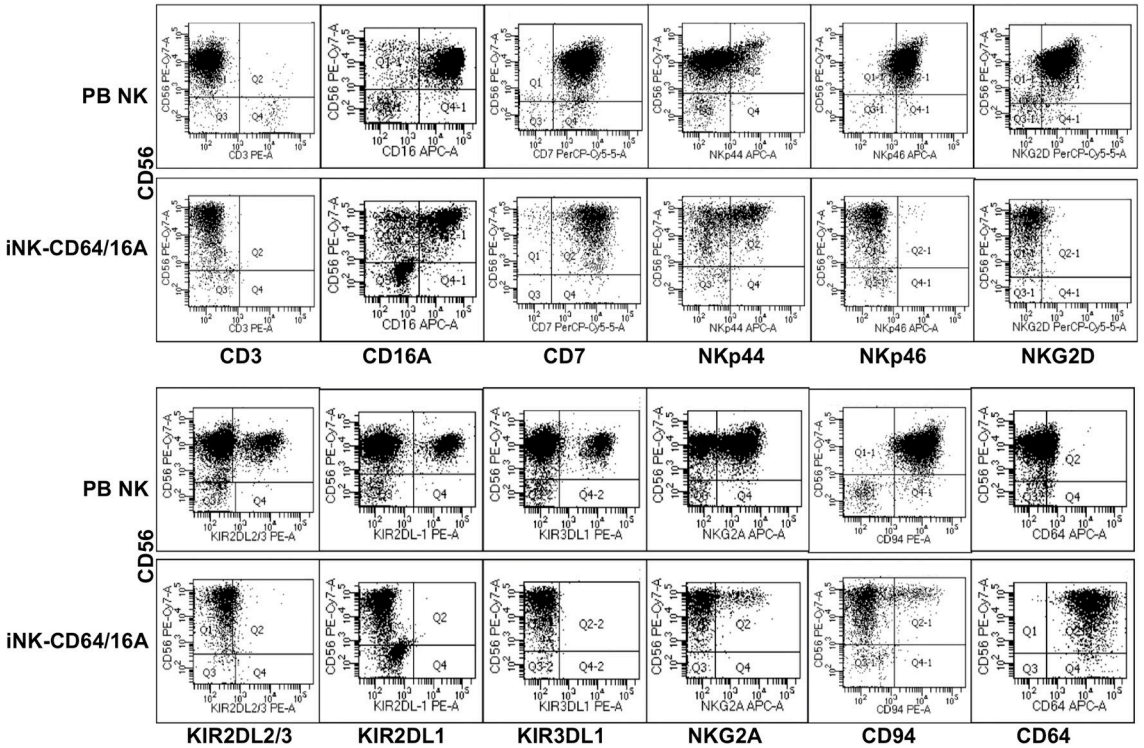

FIGURE 4 | Generation of iNK cells expressing CD64/CD16A. iPSCs were transduced to stably express CD64/16A, differentiated into NK cells, and then expanded using K562-mbIL21-41BBL feeder cells, as described in the Materials and Methods. iNK-CD64/16A cells and freshly isolated peripheral blood (PB) NK cells were stained for CD56, CD3 and various inhibitory and activating receptors, as indicated. CD64/16A expression was determined by staining the cells with an anti-CD64 mAb. For the iNK-CD64/16A cells, representative data from at least three independent experiments are shown. For the PB NK cells, three separate blood donors were examined and data from one donor is shown.

composed the majority of our differentiated cell population (**Figure 4**). We also assessed the expression of a number of activating and inhibitory receptors on the iNK cells and compared this to freshly enriched, peripheral blood NK cells. The latter cells have heterogenous phenotypes among individuals and in particular for their inhibitory receptors (39–41). In contrast to the subsets of peripheral blood NK cells expressing the inhibitory KIR receptors KIR2DL2/3, KIR2DL1, and KIR3DL1, the expanded iNK cells lacked expression of these receptors and the activating receptors NKp46 and NKG2D (**Figure 4**). Of importance is that unlike peripheral blood NK cells, essentially all of the iNK cells were stained with an anti-CD64 mAb (**Figure 4**), demonstrating the expression of CD64/16A.

To assess the function of CD64/16A, we compared iNK cells derived from iPSCs transduced with either a pKT2 empty vector or pKT2-CD64/16A. The NK cell markers mentioned above were expressed at similar levels and proportions by the two iNK cell populations (data not shown), including CD16A (**Figure 5A**), but only the iNK-CD64/16A cells were stained by an anti-CD64 mAb (**Figure 5A**). Both iNK transductants demonstrated increased SKOV-3 cell killing when in the presence of trastuzumab, yet iNK-CD64/16A cells mediated significantly higher levels of ADCC than did the iNK-pKT2 control cells (**Figure 5B**). The anti-CD16 function blocking mAb 3G8, but not the anti-CD64 mAb 10.1, effectively inhibited ADCC by the iNK-pKT2 cells (**Figure 5B**). Conversely, 10.1, but not 3G8, blocked ADCC by the iNK-CD64/16A cells (**Figure 5B**). These findings show that the generated iNK cells were cytolytic effectors responsive to CD16A and CD64/16A engagement of antibody-bound tumor cells. We also treated iNK-CD64/16A and iNK-pKT2 cells with soluble trastuzumab, washed away excess antibody, and exposed them to SKOV-3 cells. Under these conditions, ADCC by the iNK-CD64/16A cells was markedly higher than the iNK-pKT2 cells (**Figure 5C**), further establishing that CD64/16A can capture soluble anti-tumor mAbs that serve as a targeting element for tumor cell killing.

DISCUSSION

CD16A has an exclusive role in inducing ADCC by human NK cells (2–4). The affinity of antibody binding and the expression levels of this IgG Fc receptor modulate NK cell effector functions and affect the efficacy of tumor-targeting therapeutic mAbs (4, 11, 19, 20). To enhance anti-tumor antibody binding by NK cells, we expressed a novel recombinant FcγR consisting of the extracellular region of the high affinity

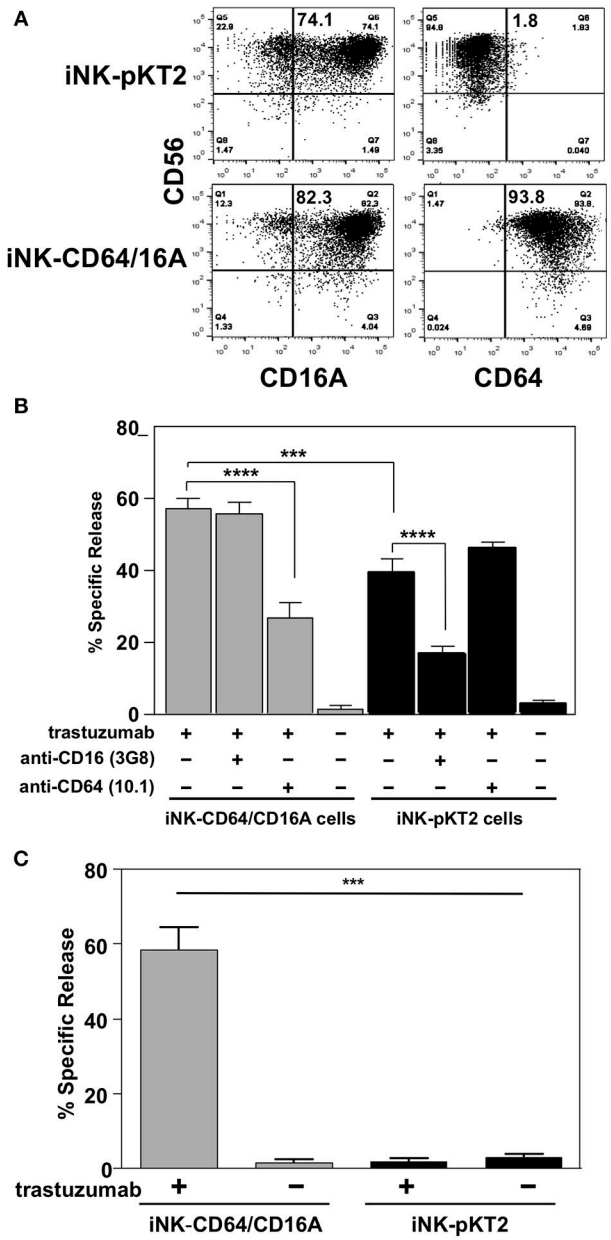

FIGURE 5 | iNK-CD64/16A cells show enhanced ADCC compared to iNK-pKT2 control cells**. (A)** iNK cells derived from empty vector (iNK-pKT2) or CD64/16A (iNK-CD64/16A) transduced iPSCs were stained for CD56, CD64, and CD16A, as indicated. The percentage of $CD56^+$ cells positively staining for CD16A or CD64 are indicated in the top right quadrant. **(B)** iNK-pKT2 or iNK-CD64/16A cells were incubated with SKOV-3 cells (E:T = 10:1; 8×10^4 cells to 8×10^3 cells) in the presence or absence of trastuzumab (5 μg/ml), the function blocking anti-CD16 mAb 3G8 (5 μg/ml), and the function blocking anti-CD64 mAb 10.1 (5 μg/ml), as indicated, for 2 h at 37°C. Data is shown as mean ± SD of three independent experiments. Statistical significance is indicated as $^{***}p < 0.001$; $^{****}p < 0.0001$. **(C)** iNK-pKT2 and iNK-CD64/16A cells were incubated in the presence or absence of trastuzumab (5 μg/ml), washed, and exposed to SKOV-3 cells (E:T = 10:1; 8×10^4 cells to 8×10^3 cells) for 2 h at 37°C. Data is shown as mean ± *SD* of three independent experiments. Statistical significance is indicated as $^{***}p < 0.001$.

FcγR CD64 and the transmembrane and intracellular regions of CD16A. NK cells expressing CD64/16A facilitated cell conjugation with antibody-bound tumor cells, cytotoxicity, and IFNγ production, demonstrating function by both components of the recombinant FcγR. CD64/16A lacks the ADAM17 cleavage region found in CD16A and it did not undergo the same level of downregulation in expression during ADCC. Moreover, consistent with the ability of CD64 to stably bind soluble monomeric IgG, NK cells expressing CD64/16A could capture soluble anti-tumor therapeutic mAbs and kill target cells.

We demonstrate that CD64/16A was functional in two human NK cell platforms, the NK92 cell line and primary NK cells derived from iPSCs. NK92 cells lack inhibitory KIR receptors and show high levels of natural cytotoxicity compared to other NK cell lines derived from patients (42). NK92 cells have been widely used to express modified genes to direct their cytolytic effector function, have been evaluated in preclinical studies, and are undergoing clinical testing in cancer patients (42, 43). iPSCs are also very amendable to genetic engineering and can be differentiated into NK cells expressing various receptors to direct their effector functions (14, 30, 37, 38). For this study, we streamlined and standardized the hematopoietic differentiation step using a commercial kit. Though the generated iNK cells lacked several inhibitory and activating receptors compared to peripheral blood NK cells and iNK cells in previous studies (29–31), the majority of the cells were $CD16A^+$, which is expressed by mature NK cells (44), and mediated ADCC, demonstrating they were cytotoxic effector cells. The particular phenotype of the iNK cells will be important for the desired effector functions. However, to better direct and enhance their anti-tumor activity through the expression of engineered receptors and reduce their off-target effects, it may be advantageous for the iNK cells not to express endogenous inhibitory and activating receptors. Tumor cell ADCC by iNK cells expressing CD64/16A cells was significantly blocked by an anti-CD64 mAb. Interestingly, in contrast to pKT2 vector control iNK cells, ADCC by the iNK-CD64/16A cells was not blocked by an anti-CD16 mAb. Why endogenous CD16A in the iNK-CD64/16A cells did not have a role in the *in vitro* ADCC assay is unclear at this time. This may be due to a competitive advantage by CD64/16A over endogenous CD16A in binding antibody and/or in utilizing the same pool of downstream signaling factors.

An individual NK cell can kill multiple tumor cells in different manners. This includes by a process of sequential contacts and degranulations, referred to as serial killing (45, 46), and by the localized dispersion of its granule contents that kills surrounding tumor cells, referred to as bystander killing (47). Further studies are required to determine the effects of CD64/16A expression on these killing processes during ADCC. Inhibiting CD16A shedding has been reported to slow NK cell detachment from target cells and reduce serial killing by NK cells *in vitro* (48). Due to the CD64 component and its lack of ectodomain shedding, NK cells expressing CD64/16A could be less efficient at serial killing

and more efficient at bystander killing. An important next step will be to assess the anti-tumor activity of NK cells expressing CD64/16A *in vivo*, which will include the use of NK92-CD64/16A cells and iNK-CD64/16A cells in tumor xenograft models.

Therapeutic mAbs have become one of the fastest growing classes of drugs, and tumor-targeting mAbs are the most widely used and characterized immunotherapy for hematologic and solid tumors (49). NK cells expressing CD64/16A have several potential advantages as a combination therapy, as their capture of anti-tumor mAbs, either individually or when mixed, prior to adoptive transfer provides diverse options for switchable targeting elements. Modifying NK cells expressing CD64/16A with an antibody would also reduce the dosage of therapeutic antibodies administered to patients. We showed that fusion proteins containing a human IgG Fc region, such as L-selectin/Fc, can also be captured by CD64/16A, which may provide further options for directing the tissue and tumor antigen targeting of engineered NK cells. Advantages of the NK92 and iNK cell platforms for adoptive cell therapies is that they can be readily gene modified on a clonal level and expanded into clinical-scalable cell numbers to produce engineered NK cells with improved effector activities as an off-the-shelf therapeutic for cancer immunotherapy (36, 37, 42, 43, 50).

AUTHOR CONTRIBUTIONS

BW and JW collected, assembled, analyzed, and interpreted the data, and wrote the manuscript. KS collected, analyzed, and interpreted the data, and revised the manuscript. RH, HM, DM, YL, and AR collected, analyzed, and interpreted the data. DK analyzed the data and revised the manuscript. All authors contributed to manuscript preparation, read, and approved the submitted version.

FUNDING

This work was supported by grants from the NIH, award numbers R01CA203348 and R21AI125729, and the Minnesota Ovarian Cancer Alliance. KS was supported by a Howard Hughes Medical Institute and Burroughs Wellcome Fund Medical Research Fellowship. AR was supported by the Office of the Director of the NIH, award number T35OD0 11118.

REFERENCES

1. Carotta S. Targeting NK cells for anticancer immunotherapy: clinical and preclinical approaches. *Front Immunol.* (2016) 7:152. doi: 10.3389/fimmu.2016.00152
2. Alderson KL, Sondel PM. Clinical cancer therapy by NK cells via antibody-dependent cell-mediated cytotoxicity. *J Biomed Biotechnol.* (2011) 2011:379123. doi: 10.1155/2011/379123
3. Long EO, Kim HS, Liu D, Peterson ME, Rajagopalan S. Controlling natural killer cell responses: integration of signals for activation and inhibition. *Annu Rev Immunol.* (2013) 31:227–58. doi: 10.1146/annurev-immunol-020711-075005
4. Wang W, Erbe AK, Hank JA, Morris ZS, Sondel PM. NK Cell-mediated antibody-dependent cellular cytotoxicity in cancer immunotherapy. *Front Immunol.* (2015) 6:368. doi: 10.3389/fimmu.2015.00368
5. Lanier LL, Yu G, Phillips JH. Co-association of CD3 zeta with a receptor (CD16) for IgG Fc on human natural killer cells. *Nature* (1989) 342:803–5. doi: 10.1038/342803a0
6. Anderson P, Caligiuri M, O'Brien C, Manley T, Ritz J, Schlossman SF. Fc gamma receptor type III (CD16) is included in the zeta NK receptor complex expressed by human natural killer cells. *Proc Natl Acad Sci USA*. (1990) 87:2274–8.
7. Letourneur O, Kennedy IC, Brini AT, Ortaldo JR, O'Shea JJ, Kinet JP. Characterization of the family of dimers associated with Fc receptors (Fc epsilon RI and Fc gamma RIII). *J Immunol.* (1991) 147:2652–6.
8. Hou X, Dietrich J, Geisler NO. The cytoplasmic tail of FcgammaRIIIAalpha is involved in signaling by the low affinity receptor for immunoglobulin G. *J Biol Chem*. (1996) 271:22815–22.
9. Li X, Baskin JG, Mangan EK, Su K, Gibson AW, Ji C, et al. The unique cytoplasmic domain of human FcgammaRIIIA regulates receptor-mediated function. *J Immunol.* (2012) 189:4284–94. doi: 10.4049/jimmunol.1200704
10. Wang Y, Wu J, Newton R, Bahaie NS, Long C, Walcheck B. ADAM17 cleaves CD16b (FcgammaRIIIb) in human neutrophils. *Biochim Biophys Acta* (2013) 1833:680–5. doi: 10.1016/j.bbamcr.2012.11.027
11. Romee R, Foley B, Lenvik T, Wang Y, Zhang B, Ankarlo D, et al. NK cell CD16 surface expression and function is regulated by a disintegrin and metalloprotease-17 (ADAM17). *Blood* (2013) 121:3599–608. doi: 10.1182/blood-2012-04-425397
12. Peruzzi G, Femnou L, Gil-Krzewska A, Borrego F, Weck J, Krzewski K, et al. Membrane-type 6 matrix metalloproteinase regulates the activation-induced downmodulation of CD16 in human primary NK cells. *J Immunol.* (2013) 191:1883–94. doi: 10.4049/jimmunol.1300313
13. Lajoie L, Congy-Jolivet N, Bolzec A, Gouilleux-Gruart V, Sicard E, Sung HC, et al. ADAM17-mediated shedding of FcgammaRIIIA on human NK cells: identification of the cleavage site and relationship with activation. *J Immunol.* (2014) 192:741–51. doi: 10.4049/jimmunol.1301024
14. Jing Y, Ni Z, Wu J, Higgins L, Markowski TW, Kaufman DS, et al. Identification of an ADAM17 cleavage region in human CD16 (FcgammaRIII) and the engineering of a non-cleavable version of the receptor in NK cells. *PLoS ONE* (2015) 10:e0121788. doi: 10.1371/journal.pone.0121788
15. Lai P, Rabinowich H, Crowley-Nowick PA, Bell MC, Mantovani G, Whiteside TL. Alterations in expression and function of signal-transducing proteins in tumor-associated T and natural killer cells in patients with ovarian carcinoma. *Clin Cancer Res.* (1996) 2:161–73.
16. Veeramani S, Wang SY, Dahle C, Blackwell S, Jacobus L, Knutson T, et al. Rituximab infusion induces NK activation in lymphoma patients with the high-affinity CD16 polymorphism. *Blood* (2011) 118:3347–9. doi: 10.1182/blood-2011-05-351411
17. Cox MC, Battella S, La Scaleia R, Pelliccia S, Di Napoli A, Porzia A, et al. Tumor-associated and immunochemotherapy-dependent long-term alterations of the peripheral blood NK cell compartment in DLBCL patients. *Oncoimmunology* (2015) 4:e990773. doi: 10.4161/2162402X.2014.990773
18. Granzin M, Soltenborn S, Muller S, Kollet J, Berg M, Cerwenka A, et al. Fully automated expansion and activation of clinical-grade natural killer cells for adoptive immunotherapy. *Cytotherapy* (2015) 17:621–32. doi: 10.1016/j.jcyt.2015.03.611
19. Felices M, Chu S, Kodal B, Bendzick L, Ryan C, Lenvik AJ, et al. IL-15 super-agonist (ALT-803) enhances natural killer (NK) cell function against ovarian cancer. *Gynecol Oncol.* (2017) 145:453–61. doi: 10.1016/j.ygyno.2017.02.028
20. Mishra HK, Pore N, Michelotti EF, Walcheck B. Anti-ADAM17 monoclonal antibody MEDI3622 increases IFNgamma production by human NK cells in the presence of antibody-bound tumor cells. *Cancer Immunol Immunother*. (2018) 67:1407–16. doi: 10.1007/s00262-018-2193-1

21. Wu J, Edberg JC, Redecha PB, Bansal V, Guyre PM, Coleman K, et al. A novel polymorphism of FcgammaRIIIa (CD16) alters receptor function and predisposes to autoimmune disease. *J Clin Invest*. (1997) 100:1059–70. doi: 10.1172/JCI119616
22. Koene HR, Kleijer M, Algra J, Roos D, von dem Borne AE, de Haas M. Fc gammaRIIIa-158V/F polymorphism influences the binding of IgG by natural killer cell Fc gammaRIIIa, independently of the Fc gammaRIIIa-48L/R/H phenotype. *Blood* (1997) 90:1109–14.
23. Dong C, Ptacek TS, Redden DT, Zhang K, Brown EE, Edberg JC, et al. Fcgamma receptor IIIa single-nucleotide polymorphisms and haplotypes affect human IgG binding and are associated with lupus nephritis in African Americans. *Arthr Rheumatol.* (2014) 66:1291–9. doi: 10.1002/art.38337
24. Nimmerjahn F, Ravetch JV. Fcgamma receptors as regulators of immune responses. *Nat Rev Immunol.* (2008) 8:34–47. doi: 10.1038/nri2206
25. Bruhns P, Iannascoli B, England P, Mancardi DA, Fernandez N, Jorieux S, et al. Specificity and affinity of human Fcgamma receptors and their polymorphic variants for human IgG subclasses. *Blood* (2009) 113:3716–25. doi: 10.1182/blood-2008-09-179754
26. Kiyoshi M, Caaveiro JM, Kawai T, Tashiro S, Ide T, Asaoka Y, et al. Structural basis for binding of human IgG1 to its high-affinity human receptor FcgammaRI. *Nat Commun*. (2015) 6:6866. doi: 10.1038/ncomms7866
27. Binyamin L, Alpaugh RK, Hughes TL, Lutz CT, Campbell KS, Weiner LM. Blocking NK cell inhibitory self-recognition promotes antibody-dependent cellular cytotoxicity in a model of anti-lymphoma therapy. *J Immunol*. (2008) 180:6392–401. doi: 10.4049/jimmunol.180.9.6392
28. Ni Z, Knorr DA, Kaufman DS. Hematopoietic and nature killer cell development from human pluripotent stem cells. *Methods Mol Biol.* (2013) 1029:33–41. doi: 10.1007/978-1-62703-478-4_3
29. Knorr DA, Ni Z, Hermanson D, Hexum MK, Bendzick L, Cooper LJ, et al. Clinical-scale derivation of natural killer cells from human pluripotent stem cells for cancer therapy. *Stem Cells Transl Med*. (2013) 2:274–83. doi: 10.5966/sctm.2012-0084
30. Ni Z, Knorr DA, Bendzick L, Allred J, Kaufman DS. Expression of chimeric receptor CD4zeta by natural killer cells derived from human pluripotent stem cells improves *in vitro* activity but does not enhance suppression of HIV infection *in vivo*. *Stem cells* (2014) 32:1021–31. doi: 10.1002/stem.1611
31. Hermanson DL, Bendzick L, Pribyl L, McCullar V, Vogel RI, Miller JS, et al. Induced pluripotent stem cell-derived natural killer cells for treatment of ovarian cancer. *Stem Cells* (2016) 34:93–101. doi: 10.1002/stem.2230
32. Woll PS, Grzywacz B, Tian X, Marcus RK, Knorr DA, Verneris MR, et al. Human embryonic stem cells differentiate into a homogeneous population of natural killer cells with potent *in vivo* antitumor activity. *Blood* (2009) 113:6094–101. doi: 10.1182/blood-2008-06-165225
33. Harrison PT, Allen JM. High affinity IgG binding by FcgammaRI (CD64) is modulated by two distinct IgSF domains and the transmembrane domain of the receptor. *Protein Eng.* (1998) 11:225–32.
34. Wang R, Jaw JJ, Stutzman NC, Zou Z, Sun PD. Natural killer cell-produced IFN-gamma and TNF-alpha induce target cell cytolysis through up-regulation of ICAM-1. *J Leukoc Biol*. (2012) 91:299–309. doi: 10.1189/jlb.0611308
35. Carlsten M, Childs RW. Genetic manipulation of NK cells for cancer immunotherapy: techniques and clinical implications. *Front Immunol.* (2015) 6:266. doi: 10.3389/fimmu.2015.00266
36. Zeng J, Tang SY, Toh LL, Wang S. Generation of "Off-the-Shelf" natural killer cells from peripheral blood cell-derived induced pluripotent stem cells. *Stem Cell Rep.* (2017) 9:1796–812. doi: 10.1016/j.stemcr.2017.10.020
37. Hermanson DL, Kaufman DS. Utilizing chimeric antigen receptors to direct natural killer cell activity. *Front Immunol.* (2015) 6:195. doi: 10.3389/fimmu.2015.00195
38. Li Y, Hermanson DL, Moriarity BS, Kaufman DS. Human iPSC-derived natural killer cells engineered with chimeric antigen receptors enhance anti-tumor activity. *Cell Stem Cell* (2018) 23:181–192.e5. doi: 10.1016/j.stem.2018.06.002
39. Strauss-Albee DM, Horowitz A, Parham P, Blish CA. Coordinated regulation of NK receptor expression in the maturing human immune system. *J Immunol*. (2014) 193:4871–9. doi: 10.4049/jimmunol.1401821
40. Horowitz A, Strauss-Albee DM, Leipold M, Kubo J, Nemat-Gorgani N, Dogan OC, et al. Genetic and environmental determinants of human NK cell diversity revealed by mass cytometry. *Sci Transl Med*. (2013) 5:208ra145. doi: 10.1126/scitranslmed.3006702
41. Strauss-Albee DM, Fukuyama J, Liang EC, Yao Y, Jarrell JA, Drake AL, et al. Human NK cell repertoire diversity reflects immune experience and correlates with viral susceptibility. *Sci Transl Med*. (2015) 7:297ra115. doi: 10.1126/scitranslmed.aac5722
42. Klingemann H, Boissel L, Toneguzzo F. Natural killer cells for immunotherapy - advantages of the NK-92 cell line over blood NK Cells. *Front Immunol.* (2016) 7:91. doi: 10.3389/fimmu.2016.00091
43. Zhang C, Oberoi P, Oelsner S, Waldmann A, Lindner A, Tonn T, et al. Chimeric antigen receptor-engineered NK-92 Cells: an off-the-shelf cellular therapeutic for targeted elimination of cancer cells and induction of protective antitumor immunity. *Front Immunol.* (2017) 8:533. doi: 10.3389/fimmu.2017.00533
44. Seidel UJ, Schlegel P, Lang P. Natural killer cell mediated antibody-dependent cellular cytotoxicity in tumor immunotherapy with therapeutic antibodies. *Front Immunol.* (2013) 4:76. doi: 10.3389/fimmu.2013.00076
45. Bhat R, Watzl C. Serial killing of tumor cells by human natural killer cells–enhancement by therapeutic antibodies. *PLoS ONE* (2007) 2:e326. doi: 10.1371/journal.pone.0000326
46. Vanherberghen B, Olofsson PE, Forslund E, Sternberg-Simon M, Khorshidi MA, Pacouret S, et al. Classification of human natural killer cells based on migration behavior and cytotoxic response. *Blood* (2013) 121:1326–34. doi: 10.1182/blood-2012-06-439851
47. Hsu HT, Mace EM, Carisey AF, Viswanath DI, Christakou AE, Wiklund M, et al. NK cells converge lytic granules to promote cytotoxicity and prevent bystander killing. *J Cell Biol.* (2016) 215:875–89. doi: 10.1083/jcb.201604136
48. Srpan K, Ambrose A, Karampatzakis A, Saeed M, Cartwright ANR, Guldevall K, et al. Shedding of CD16 disassembles the NK cell immune synapse and boosts serial engagement of target cells. *J Cell Biol*. (2018) 217:3267. doi: 10.1083/jcb.201712085
49. Battella S, Cox MC, Santoni A, Palmieri G. Natural killer (NK) cells and anti-tumor therapeutic mAb: unexplored interactions. *J Leukoc Biol*. (2016) 99:87–96. doi: 10.1189/jlb.5VMR0415-141R
50. Angelos MG, Kaufman DS. Pluripotent stem cell applications for regenerative medicine. *Curr Opin Organ Transplant*. (2015) 20:663–70. doi: 10.1097/MOT.0000000000000244

Conflict of Interest Statement: The authors declare that the research was conducted in the absence of any commercial or financial relationships that could be construed as a potential conflict of interest.